First-principles calculations of MnB_2, TcB_2, and ReB_2 within the ReB_2-type structure

Sezgin Aydin and Mehmet Simsek
Department of Physics, Faculty of Arts and Sciences, Gazi University, 06500 Teknikokullar, Ankara, Turkey
(Received 19 December 2008; revised manuscript received 13 August 2009; published 6 October 2009)

The structural, mechanical, and electronic properties of MnB_2, TcB_2, and ReB_2 have been studied by performing first-principles calculations at the level plane-wave basis pseudopotential formalism in both aluminum diboride- and rhenium diboride-type structures. The results of local density approximation and generalized gradient approximation indicated that all three of hexagonal structures within rhenium diboride-type are energetically favorable than those of aluminum diboride-type, they are mechanically stable and also hard materials. In addition to electronic properties of highly directional covalent bonds, optimal filling of bonding states, mechanical properties, and also the Debye temperature of the structures support that the rhenium diboride-type hexagonal phase of MnB_2 is harder than the others. Interestingly, instead of other five structures, only MnB_2 within aluminum diboride-type hexagonal structure has a finite magnetic moment at the equilibrium geometry.

DOI: 10.1103/PhysRevB.80.134107 PACS number(s): 62.20.−x, 71.15.Mb, 71.20.−b, 83.60.−a

I. INTRODUCTION

Recently, the investigation of superhard materials has attracted much interest,[1–5] because of their importance in science, technology, and industrial applications. Therefore, considerable efforts have been devoted to design and syntheses new superhard materials,[1–10] as hard as or even harder than diamond, cubic boron nitride (BN), boron carbide (B_4C), and/or cubic BC_2N. Meantime, some groups of scientists offered the new types of potential superhard materials[5–9] which contain heavy transition metal atoms and strong covalent bonding atoms such as B, C, N, and O. According to their conclusions, transition metal borides, carbides, nitrides, and oxides might be very hard materials.[5–13]

Recently, Cynn *et al.*[14] measured the bulk modulus of solid osmium as 462 ± 12 GPa, which is higher than that of diamond (443 GPa); their finding initiated an increased interest to transition metals and their compounds with light elements.[15–21] Due to the high valance electron density (0.572 electrons/Å^3) and least compressibility of Os, osmium borides, nitrides, and/or oxides have been extensively studied.[6–8,13,18–22] However, it is interesting appeared that none of them was superhard material,[18] and also the hardnesses of osmium[18] and osmium diboride[8] were 4.0 and 27.9 GPa, respectively.

Kaner, Gilman and Tolbert[4,5] suggested the design principles of a new superhard material to overcome the dream of exceeding the hardness of diamond. Chung *et al.*[17] have recently synthesized ReB_2, which has super-incompressibility and high hardness with a casting techniques at ambient pressure. Although hexagonal ReB_2 has a metallic structure, it seems to be a superhard material. On the other hand, Dubrovinskaia *et al.*[23] commenting on the work of Chung *et al.*,[17] they noted that ReB_2 was not a superhard material. In the response to the comment of Dubrovinskaia *et al.*,[23] Chung *et al.*[24] presented an AFM profile of scratch marc on the diamond surface.

More recently, two experimental results about ReB_2 have been presented by Locci *et al.*[25] and Otani *et al.*[26] Locci *et al.* used the spark plasma sintering techniques and Otani *et al.* used self-propagation high-temperature reaction techniques. In both experiments, the measured Vickers microhardness of ReB_2 was within the limit (40 GPa). On the other hand, Wang[28] pointed out that the ReB_2-type hexagonal structures of TcB_2 and ReB_2 were more stable than the orthorhombic form. However, the calculated electronic properties, large elastic modulus, and large G/B values signified that both hexagonal structures are potential superhard materials. In the recent first-principles calculation[27] it has been reported that, instead of orthorhombic and AlB_2-type structures of ReB_2, ReB_2-type structure was energetically favorable. Lian and Zang[29] also calculated the mechanical and electronic properties of ReB_2, and they concluded that the effect of spin-orbit coupling is significantly important, and ReB_2 was ultraincompressible and it might be potential superhard material. Meantime, Zhou *et al.*[30] have applied density functional theory and neutron scattering techniques to find the electronic, elastic, phonon, and thermal properties of ReB_2. They indicated that strongly covalent B–B bonds and Re–B bonds have been played critical role in the incompressibility and hardness, hence, ReB_2 might be a potential superhard material. Furthermore, Hao *et al.*[31] studied structural, elastic and electronic properties of ReB_2 and WB_2, and their suggestion was that hexagonal structures of ReB_2 and WB_2 were potential low compressible and hard materials. Zhu *et al.*[32] also calculated the structural parameters and elastic properties of ReB_2 under pressure; according to their result it was a sort of low compressible and an anisotropic material. Wang *et al.*,[33] in their first-principles calculations, suggested that WB_4 and other five compounds ReB_4, TaB_4, MoB_4, TcB_4, and OsB_4 within WB_4 structure might be superhard materials.

On the other hand, the borides of manganese are well known for a long time.[34] Structural, and magnetic properties of hexagonal MnB_2 (within AlB_2-type structure) have been studied more than four decades.[35–37] However, Cely *et al.*[38] synthesized different Mn-B compounds by arc melting technique, and measured their microhardness and structural properties. Armstrong[39] examined the electronic structure of the first-row transition metal diborides, and they showed that while moving from ScB_2 to the MnB_2, the ionic bonding and the boron-boron bonding become smaller. Moreover, elec-

tronic structures, bonding, and ground-state properties of MnB_2 within AlB_2-type structure, and other transition metal borides have been investigated.[40]

In this study, we systematically investigated ReB_2-type hexagonal structures of VIIB group of element-diboride compounds, such as MnB_2, TcB_2 and ReB_2 by using density functional theory method. AlB_2-type hexagonal structures are optimized at the ground state. Spin-polarization and magnetovolume effects are also calculated. The following section (Sec. II) contains technical details of the first-principles calculations, such as computational methods of geometry optimizations, elastic properties, brief review of the method of hardness calculation, and also the relationship of the Debye temperature hardness of materials. In the results and discussion section (Sec. III), the details of bonding characters, mechanical and magnetic properties of all six of phases are discussed. The conclusions are presented in the last section (Sec. IV).

II. METHOD OF CALCULATIONS

A. Geometry optimization

In the first stage of the calculations the equilibrium geometries of the systems studied (MnB_2, TcB_2, and ReB_2) have been obtained, then the mechanical and electronic properties of them calculated by using density functional theory method within the CASTEP code.[41] The calculations were performed on a $14\times14\times8$ Monkhorst-Pack grid. The exchange-correlation functional was taken into account through generalized gradient approximation (GGA) (Ref. 42) and Perdew Burke Ernzerhof functionals (PBE).[43] The interactions between the ions and the electrons were described by using the Ultrasoft Vanderbilt pseudopotentials.[44] Local density approximation (LDA) (Ref. 45) was also used to test the ground states of the structures in the equilibrium conditions. To speed up convergence with respect to the ultrafine setup of the code for Broyden, Fletcher, Goldfarb, Shanno (BFGS) minimization, two different cutoffs for the plane-wave basis set were chosen, one for MnB_2 and ReB_2: 310 eV, and the other one for TcB_2: 320 eV. Two different strategies have been followed in the optimization stage. First, the initial structures of MnB_2, TcB_2, and ReB_2 were chosen in the form of rhenium diboride-type hexagonal lattice ($P6_3/mmc$ space group, No 194). This structure is well-known in the literature.[46] Second, the aluminum diboride-type (AlB_2) hexagonal lattices (P6/mmm space group, No 191) for all three structures (MnB_2, TcB_2, and ReB_2) have been chosen as initial structure.

After optimizations, energy-volume curves were drawn for six different structures for comparison. Mechanical properties such as hardness, elastic constants, C_{ij}, bulk modulus, shear modulus, and the Debye temperatures were calculated. Furthermore, from 0 GPa to 30 GPa geometry optimizations were also performed under hydrostatic pressure.

We note that structural,[34,35,38] magnetic,[36,37,47] and electronic[39,40] properties of AlB_2-type of MnB_2 have been investigated previously. In addition to these we also calculated spin- polarization effects for the structures (MnB_2, TcB_2, and ReB_2) in both types.

B. Elastic properties

In order to find elastic constants of a structure, a small strain is applied onto the structure then the change in energy or stress can be calculated in the structure. If the primitive cell volume of crystal has a small strain ε, the total energy $E(V,\varepsilon)$ can be expanded as a Taylor series,[48]

$$E(V,\varepsilon) = E(V_0,0) + V_0\sum_{i=1}^{6}\sigma_i\varepsilon_i + \frac{V_0}{2}\sum_{i=1}^{6}c_{ij}e_ie_j + \cdots, \quad (1)$$

where $E(V_0,0)$ is the energy of the unstrained system with the equilibrium volume V_0, ε is strain tensor which is defined as[48]

$$\varepsilon = \begin{pmatrix} e_1 & \frac{1}{2}e_6 & \frac{1}{2}e_5 \\ \frac{1}{2}e_6 & e_2 & \frac{1}{2}e_4 \\ \frac{1}{2}e_5 & \frac{1}{2}e_4 & e_3 \end{pmatrix} \quad (2)$$

and c_{ij} are the elastic constants, which are response to an applied stress. Both stress and strain have three tensile and three shear components. The elastic constants form a 6×6 symmetric matrix.[31]

We note that, there are five independent elastic constants (c_{11}, c_{12}, c_{13}, c_{33}, and c_{44}) for hexagonal structures. In the CASTEP calculations, the distorted structures are automatically generated and compared with the ideal (initial) structure to calculate strain sand stress. On the other hand, bulk modulus is calculated as the function of elastic constants, instead of from the second derivative of total energy, which corresponds to the Reuss bulk modulus. However, in experimental measurements, single-crystal properties of transition metal diborides may not be stand for their mechanical properties, so we used the Voigt-Reuss-Hill approximation,[49] assuming to be constant local intergrain stresses of polycrystalline materials. The following formulation is useful to calculate the bulk and shear modulus of the polycrystalline hexagonal structures. In this approximation,[48,49] the Voigt bulk modulus (B_V) and the shear modulus (G_V) are given as the functions of elastic constants,[31]

$$B_V = \frac{1}{9}[2(c_{11}+c_{12}) + 4c_{13} + c_{33}], \quad (3a)$$

$$G_V = \frac{1}{30}[M + 12c_{44} + 12c_{66}]. \quad (3b)$$

The Reuss bulk modulus (B_R) and the shear modulus (G_R) are defined as,

$$B_R = C^2/M, \quad (4a)$$

$$G_R = \frac{5}{2}(C^2c_{44}c_{66})/[3B_Vc_{44}c_{66} + C^2(c_{44}+c_{66})], \quad (4b)$$

where, $C^2=(c_{11}+c_{12})c_{33}-2c_{13}^2$, $M=c_{11}+c_{12}+2c_{33}-4c_{13}$, and, $c_{66}=(c_{11}-c_{12})/2$.

In considering the Hill empirical approximation,[49] the modulus is average of Reuss and Voigt moduli, namely, for a material the bulk modulus (B) and shear modulus (G) are simply expressed as

$$B = (B_V + B_R)/2, \tag{5a}$$

$$G = (G_V + G_R)/2. \tag{5b}$$

The Young modulus and Poisson ratio are calculated from the following equations:[48]

$$E = 9BG/(3B + G), \tag{6a}$$

$$\upsilon = (3B - 2G)/2(3B + G). \tag{6b}$$

C. Hardness

According to the hardness conditions,[4,5] shorter interatomic distances, smaller number of nearest neighbors, highly directional bonding, etc., increase the hardness of the crystal structures. In order to make an accurate calculation or characterization about the hardness, a theoretical hardness method should quantitatively include these basic conditions. Furthermore, when the structures are contain two or more kinds of bonds, such as in the compounds of transition metal and light atoms, it should be include not only pure covalent bond characters but also ionic bond characters. On the other hand, the hardness is closely related to anisotropy and the indenter orientation in the structures.[50] Nevertheless, to the knowledge of authors, there is no general calculation method involving hardness anisotropies in different dimensions, however, recently a semiempirical method of hardness was developed by Simunek and Vackar[22,51] in the concept of atomistic and bond strengths properties. The method based on the atomic properties and bond strengths, and it was successfully tested by the authors on the more than 30 binary structures with zinc blende and rock salt crystals, and also for highly covalent crystals.[22,51] It was also shown that the method could have been applied to the crystals involving covalent and ionic bonding characters, and generalized to the complex structures with more than two different bond strengths.[22,51] In the same studies, it was also reported that for the covalent crystals, there are agreements between their results and those of another hardness method of Gao and co-workers[52,53] Therefore, in view of these qualitative and quantitative properties, the hardness of optimized hexagonal structures of transition metal diborides can be calculated by the method of Simunek and Vackar.[22,51] In this method, the hardness of a material is defined in general form as

$$H = \frac{C}{\Omega} n \left[\prod_{i,j=1}^{n} N_{ij} S_{ij} \right]^{1/n} e^{-\sigma f_e}, \tag{7}$$

$$f_e = 1 - \left[k(\prod_{i=1}^{k} e_i)^{1/k} / \sum_{i=1}^{k} e_i \right]^2. \tag{8}$$

where, C and σ are constants, Ω is volume of the unit cell, n denotes the number of different kind of bonds, k corresponds to the number of atoms, and the number N_{ij} counts interatomic bonds in the unit cell. S_{ij} is bond strength of d_{ij} length between atoms i and j, and defined as,

$$S_{ij} = \sqrt{e_i e_j}/(n_i n_j d_{ij}), \tag{9}$$

where $e_i = Z_i/R_i$, and Z_i is the valance electron number and R_i is atomic radius of the atom i. In the present study, in the hardness calculations the atomic radii for different elements were taken from Pearson's text book.[54] The constant values $C = 1450$ and $\sigma = 2.8$ were chosen as in the work of Simunek's,[51] these values were determined from the sufficient results of many measured hardness values of zinc blende and rock salt structures. Those constants were used before in the literature[22,51] and they gave reliable results for the structures of more than one bond strength such as diamondlike tetragonal structure, nitride spinel materials, aluminum diboride, rhenium diboride, osmium diboride, etc.

D. Debye temperature-hardness relation

Mechanical properties can also be related to thermodynamical parameters especially specific heat, thermal expansion, Debye temperature, melting point, etc.[31,55] In this concept, Debye temperature is one of fundamental parameters for the characterization of the materials[56] and the microhardness of a solid, which is dimensionally reciprocal to the compressibility.[57] According to the theory of Abrahams and Hsu,[57] there is a relationship between Debye temperature and Vickers hardness of materials, suggested by the following empirical relation:[57]

$$\theta_D \propto H^{1/2} \Omega^{1/6} M^{-1/2}, \tag{10}$$

where M is molar mass, Ω is molecular volume and H is Vickers hardness. On the other hand, there is a relation between the Debye temperature and the average sound wave velocity as,[55]

$$\theta_D = \frac{h}{k_B} \left(\frac{3n}{4\pi\Omega} \right)^{1/3} \upsilon_m, \tag{11}$$

where h and k_B are Planck and Boltzmann constants, respectively, and n is the number of atoms in the molecule. The average sound wave velocity (υ_m) is approximately given as,[31]

$$\upsilon_m = \left[\frac{1}{3} \left(\frac{2}{\upsilon_t^3} + \frac{1}{\upsilon_l^3} \right) \right]^{-1/3}, \tag{12}$$

where υ_t and υ_l are transverse, $\upsilon_t = \sqrt{G/\rho}$ and longitudinal, $\upsilon_l = \sqrt{(3B+4G)/3\rho}$ elastic sound velocities of the polycrystalline materials, respectively.

III. RESULTS AND DISCUSSION

In the first stage, the ground-state structures of MnB_2, TcB_2, and ReB_2 were obtained by performing LDA and GGA calculations with/without spin-polarization effects. As seen in Figs. 1(a)–1(c), ReB_2-type structures of all three materials (MnB_2, TcB_2, and ReB_2) have lower total energies

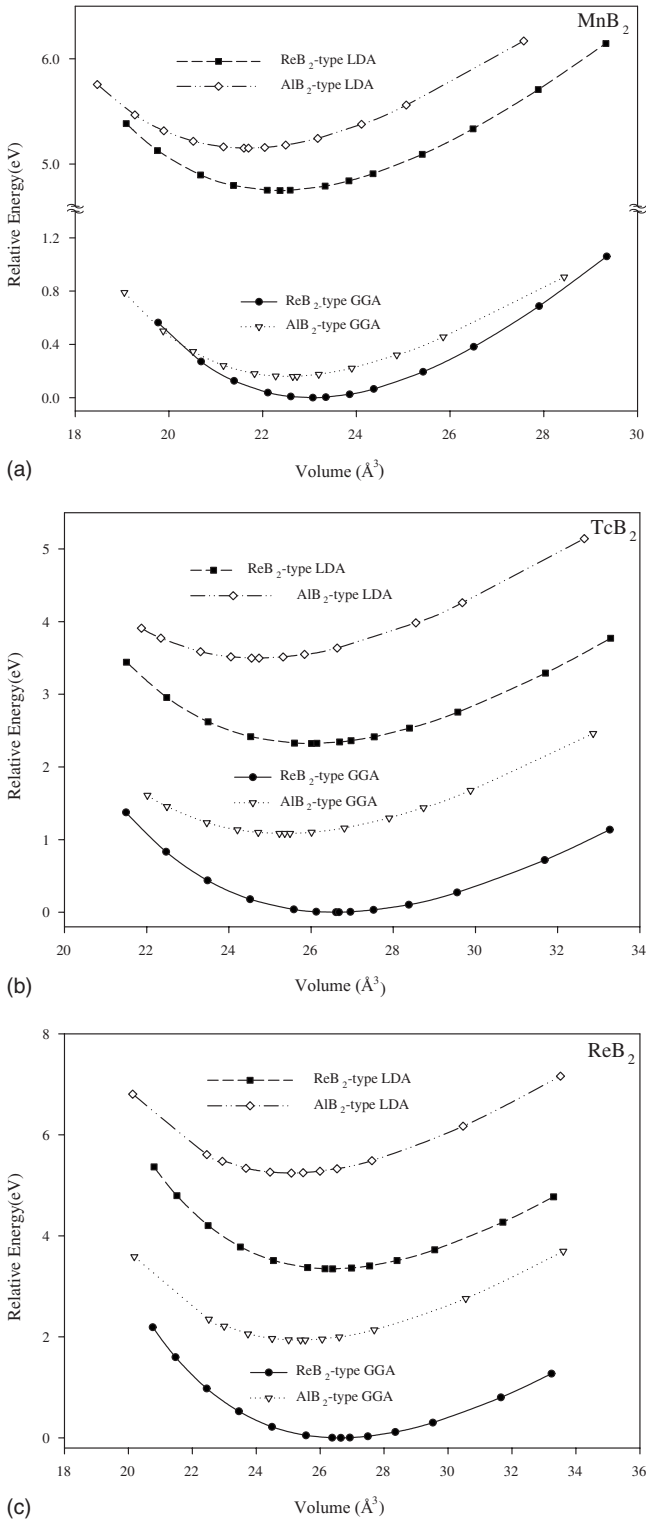

FIG. 1. The calculated relative energy-volume curves of the unit cell within ReB_2-type and AlB_2-type for LDA and GGA approximations. (a) MnB_2, (b) TcB_2, and (c) ReB_2.

than those of AlB_2-types, thus they are believed to be in their ground states.

After obtaining the ground-state structures, the structural parameters, bonding mechanisms, electronic properties, elastic constants, Vickers microhardness, and Debye temperature

TABLE I. The calculated structural parameters and cohesive energies per formula unit of MnB_2, TcB_2, and ReB_2 compared with other theoretical and experimental data.

Parameter	MnB_2	TcB_2	ReB_2
a (Å)	2.769	2.877	2.880
			2.872[a]
			2.874[b]
			2.881[c]
			2.900[d]
			2.880[e]
c (Å)	6.949	7.421	7.420
			7.405[a]
			7.412[b]
			7.410[c]
			7.478[d]
			7.423[e]
a/c	0.398	0.388	0.388
			0.388[e]
V (Å^3)	46.14	53.21	53.29
			53.318[e]
Density (g/cm^3)	5.51	7.52	12.95
			12.68[d]
			12.67[f]
Cohesive energy f.u. (eV)	−14.279	−14.044	−14.736

[a]Reference 29.
[b]Reference 29 with SOC +relaxed.
[c]Reference 31.
[d]References 17 and 46.
[e]Reference 32.
[f]Reference 25.

are calculated. The equilibrium lattice constants, volumes, densities, and cohesive energies for ReB_2-type structures are listed in Table I. As seen from the Table I, all three of hexagonal structures are in similar geometry. While ReB_2 has the highest density, highest lattice parameters, and volume, MnB_2 has the smallest ones. The results for ReB_2 agree well with experimental and other theoretical data but, for the other candidates, MnB_2 and TcB_2, however, we could not intriguing comparison experimental and theoretical data. Therefore, we hope that the obtained results for ReB_2-type MnB_2 and TcB_2 in this work may give useful information for further experimental and theoretical studies.

For discussion of bonding mechanism of the structures, we have calculated Mulliken bond populations and bond lengths in unit lattices of MnB_2, TcB_2, and ReB_2, and then plotted corresponding electron density maps in Figs. 2(a)–2(c). The results for Mulliken populations are given in Table II with the other data. Chemically, the positive Mulliken population values correspond to bonding character and negative values are antibonding character of the structures.

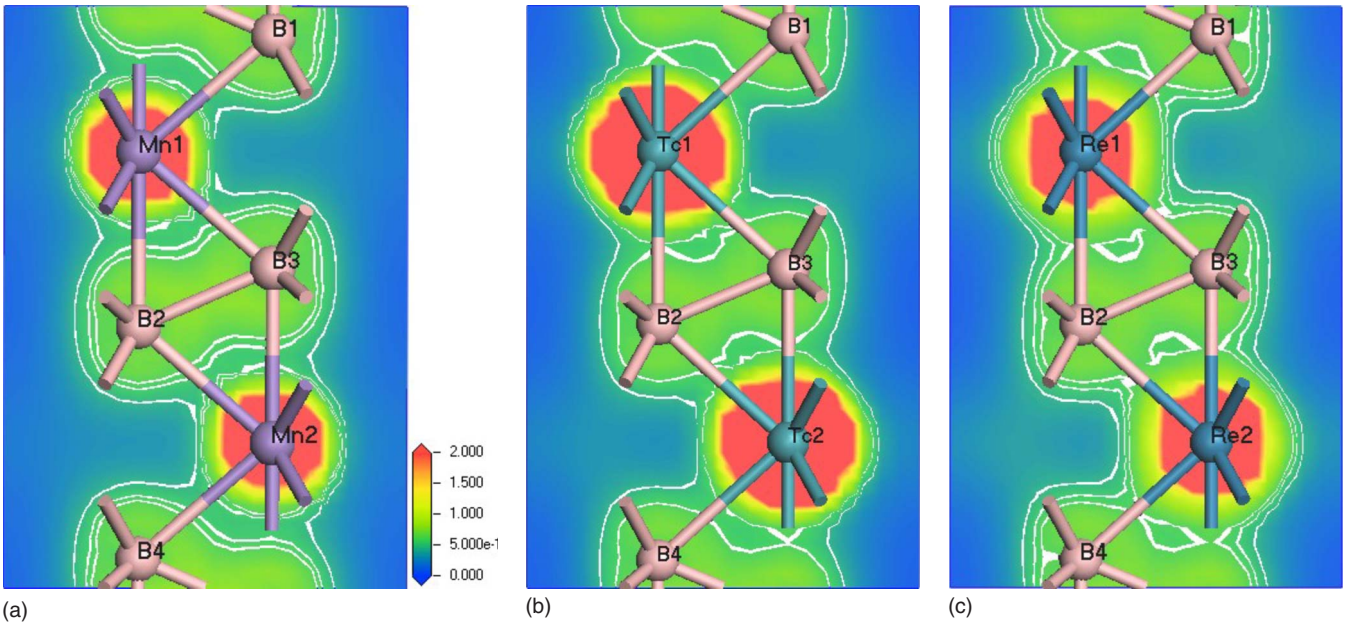

FIG. 2. (Color online) The electron density maps for (a) MnB_2, (b) TcB_2, and (c) ReB_2 in-plane (110). B1, B2, B3, B4, and M1, M2 atoms are in the same plane (110). Bn ($n=1,2,3,4$) and M1, M2 stand for boron atoms and transition metal atoms, respectively.

Furthermore, if the value of Mulliken bond population is close to zero, ionic interaction increases between two atoms forming the bond. Generally, a high value of positive population indicates a high degree of covalency in the bond.[58] This situation can easily be seen from the plotted electron density maps (see Fig. 2). As seen in Table II, Mulliken bond population is correlated with the large electron densities between two nearest boron atoms, and also between the transition metal atoms M (Mn, Tc, or Re) and their neighboring boron atoms.

It should be note that, in the rhenium diboride-type hexagonal lattice, transition metal atoms are accommodated as alternating layers, in the (00*l*) planes, of hexagonal close packed and puckered hexagonal networks of boron atoms. Every transition metal atom has eight neighboring boron atoms, and each boron atom, which is located between the layers, has four neighboring transition metal atoms and three neighboring boron atoms. As seen in Fig. 2, and Table II, two different bonding characters take place in both interactions, B–B and M–B, i.e., one group of B–B and M–B bonds are covalent, and the other ones are ionic. It is interesting to note that, although all bonds between M and B atoms, and also between B atoms are out of the plane (00*l*), in which the bonds across (along) to the *c* axis have positive (negative) Mulliken bond populations in all the three structures. As indicated in Ref. 27, zigzag B–M and B–B covalent bonds connect local buckled B layers. However, B–B bonds between nearest boron atoms [in the (110) plane] are very strong and highly covalent in all the three structures, and among them, the shortest bond length (d=1.744 Å) and the highest population (2.27) exist for MnB_2 structure. Moreover, all negative (antibonding) populations located on the bonds of B–B and M–B are directionally, along to the *c* axis. Thus, there is very weak antibonding interaction boron to second nearest boron atoms, distances far from 2.778 Å (for MnB_2) to 3.007 Å (for ReB_2).

TABLE II. The calculated Mulliken bond populations and bond lengths (in Å) in ReB_2-type MnB_2, TcB_2, and ReB_2.

	MnB_2		TcB_2		ReB_2	
	Population	Length	Population	Length	Population	Length
B–B	2.27	1.744	2.09	1.800	1.93	1.805
					1.96[a]	1.820[a]
M–B	0.30	2.118	0.57	2.244	0.73	2.242
					0.72[a]	2.257[a]
M–B	−0.31	2.086	−0.29	2.202	−0.24	2.206
					−0.25 [a]	2.227[a]
B–B	−0.06	2.778	−0.09	3.018	−0.13	3.007
					−0.14 [a]	3.025[a]

[a]Reference 30.

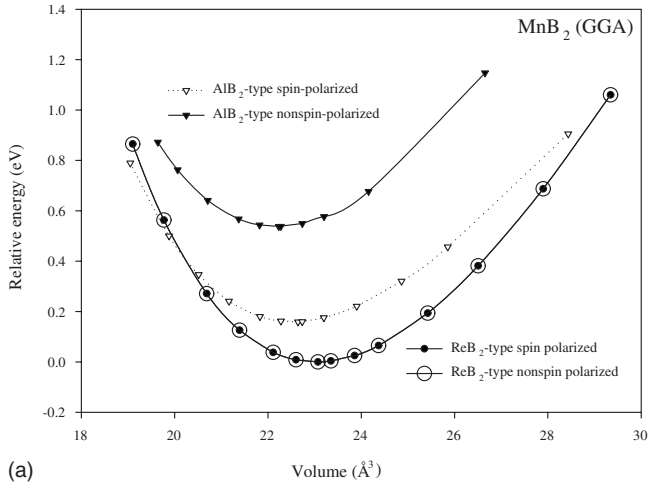

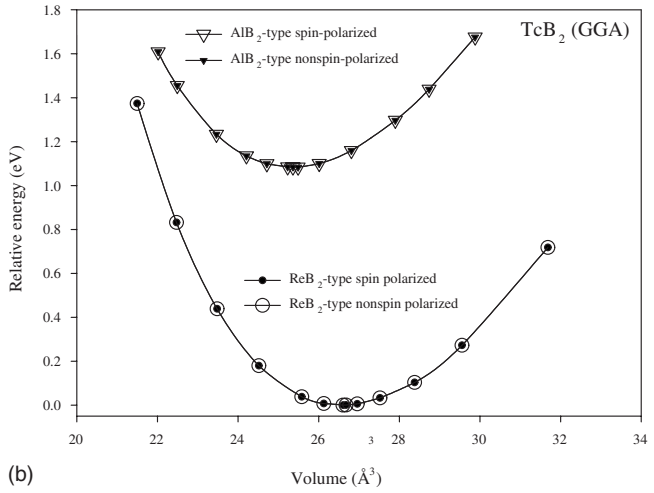

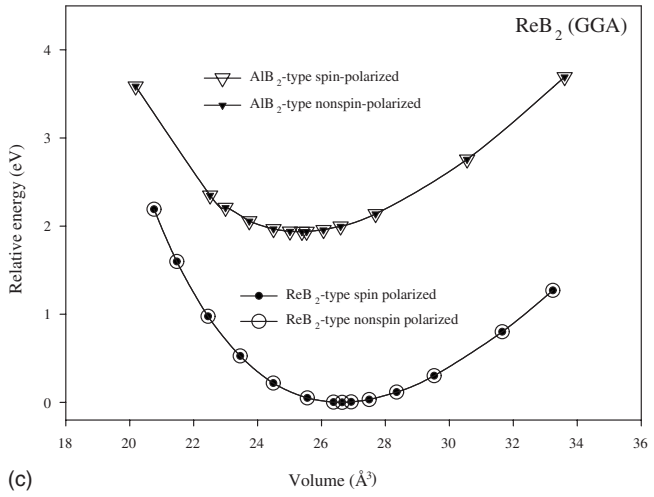

FIG. 3. The calculated relative energy-volume curves for (a) MnB_2, (b) TcB_2, and (c) ReB_2 from the spin-polarized and nonspin-polarized calculations within GGA approximation.

The spin-polarization effects on two types of hexagonal structures (in the ReB_2-type and AlB_2-type) are also calculated. It can be seen from Figs. 3(a)–3(c) that total energy-volume curves of all three structures in the ReB_2-type and also in the AlB_2-type structures of TcB_2 and ReB_2 (except

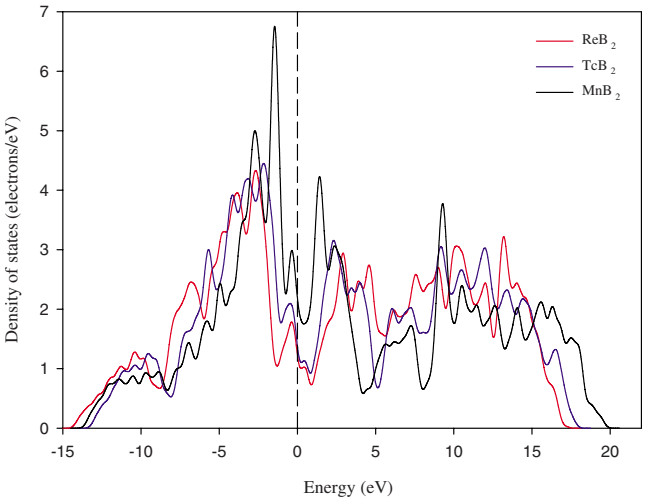

FIG. 4. (Color online) Total DOSs of MnB_2, TcB_2, and ReB_2. The vertical dashed line at zero is the Fermi energy level.

MnB_2) are nonspin polarized materials at their equilibrium geometry. Hence, integrating total spin up and spin down density of states (DOS) to Fermi energy level for MnB_2 in the AlB_2-type, magnetic moment of the structure can be found. The calculated magnetic moment for AlB_2-type MnB_2 is $1.999\mu_B$/Mn and $1.682\mu_B$/Mn for GGA and LDA approximations, respectively. If the orbital moment was assumed frozen, as in the Ref. 47, the corresponding absolute spin value of the Mn atom is $S(=\mu/2)$. Then, the effective magnetic moment can be calculated as $\mu_{eff}=2\mu_B\sqrt{S(S+1)} \cong 2.83\mu_B$ ($2.49\mu_B$) for GGA (LDA) calculations, which are agree well with the other results ($2.3\mu_B$,[59] $2.6\mu_B$,[37] $2.8\mu_B$),[47] $3.0\mu_B$.[60] According to the classification of magnetic materials, it seems to be a ferromagnetic. We note that all these values are far from the early experimental result ($0.19\mu_B$/Mn) of Andersson *et al.*[36]

Figure 4 shows the total density of states of MnB_2, TcB_2, and ReB_2. The graphs of the DOSs show that all three of materials are metallic. Because of strong covalency in the bonds of B–B, and partially covalency of M (Mn, Tc, Re) –B, the bond states are generally localized near the Fermi level, in which highest ones are for MnB_2. On the other hand, according to band filling theory,[61,62] if the number of bonding (antibonding) states increase (decrease), the stability of a material increases. Thus, the ratio W_{occ} (the width of the occupied states)/W_{b}(the width of the bonding states) may give information about the stability of the material. If the value of ratio is closer to 1.0, the stability increases. To investigate the stability of the structures, the pseudogaps (W_{p}, the nearest valley to the Fermi level), occupation gaps (W_{occ}), bonding gaps (W_{b}) and the $W_{\mathrm{occ}}/W_{\mathrm{b}}$ ratios are given in Table III for all three structures. From Table III, according to the band filling theory, because of $W_{\mathrm{occ}}/W_{\mathrm{b}}=0.972$ is closer to 1.0 than that of TcB_2 (0.945), and ReB_2 (0.944), MnB_2 seems to be the most stable material. Additionally, as seen in Fig. 4, the pseudogaps for all three of structures falls above the Fermi energy level, namely, all the bonding states are not filled and some extra electrons are required to reach the maximum stability.

The calculated elastic constants of MnB_2, TcB_2, and ReB_2 were tabulated in Table IV together with their corresponding

TABLE III. The width of occupied states W_{occ} (eV), bonding states W_b (eV), and W_{occ}/W_b of MnB_2, TcB_2, and ReB_2.

	Pseudogap (eV)	W_{occ}	W_b	W_{occ}/W_b
MnB_2	0.412	14.462	14.874	0.972
TcB_2	0.816	14.052	14.867	0.945
ReB_2	0.903	15.191	16.094	0.944

previous theoretical and experimental results. For a stable hexagonal structure, there are five independent elastic constants (c_{11}, c_{12}, c_{13}, c_{33}, and c_{44}) and they should satisfy Born stability criteria,[64] namely, $c_{12}>0$, $c_{33}>0$, $c_{66}=(c_{11}-c_{12})/2>0$, $(c_{11}+c_{12})c_{33}-2c_{13}^2>0$. As seen in Table IV, the calculated elastic constants of MnB_2, TcB_2, and ReB_2 satisfy the Born stability criteria,[64] so all three of hexagonal structure are mechanically stable.

When the structures are considered separately, c_{33} has the highest value among the elastic constants in each structure, 1081 GPa for ReB_2, 937 GPa for TcB_2, and 895 GPa for MnB_2. This shows that the hardness of ReB_2-type structures along the c axis is larger than that of other directions. At the same time, the large c_{33} values indicate unusually high incompressibility in direction of c axis. For the other elastic constants, c_{11} indicates deformation along the a axis,[27] the c_{12} and c_{13} relate to the Poisson effect in the hexagonal structures.[65] The elastic constant c_{44} relates to the monoclinic shear distortion in the (100) planes,[28] which includes four M–B bonds in ReB_2-type structures, and the c_{66} relates to the resistance to shear in the ⟨110⟩ direction.[65] In all three materials, the lowest value of c_{44} (251 GPa.) is that of TcB_2, and the lowest value of c_{66} (169 GPa.) is that of MnB_2. Furthermore, the shear anisotropy ratio (A), which is defined as c_{44}/c_{66}, the values of all three of structures are also listed in Table IV. All of them are larger than 1.0, and that of MnB_2 is the largest (1.65).

Using the Eqs. (3a), (3b), (4a), (4b), (5a), (5b), (6a), and (6b), the bulk and shear moduli, young moduli, G/B ratios and Poisson ratios of MnB_2, TcB_2, and ReB_2 are calculated. The elastic properties, which are the functions of the elastic constants of the material, tabulated in Table V with the other related data. In order to see relationships between hardness and these parameters, the hardness data are also listed in there. From Table V, bulk modulus, shear modulus, young modulus, and also G/B ratio for MnB_2 are equal or smaller than that of the other two structures. However, the hardness ($\approx$44 GPa) and the Poisson ratio (0.18) of MnB_2 are slightly larger than those of TcB_2 and ReB_2. It is interesting note that, although bulk modulus $B[=(c_{11}+2c_{12})/3]$ and shear modulus $G(=c_{44})$ are the most important indicator parameters of hardness in cubic structure of transition metal nitrides and carbides,[11] for hexagonal structures of transition metal diboride compounds, bulk and/or shear modulus are not exactly correlate to their hardness.

Although Chung *et al.*[17] obtained recently the average Vickers hardness for ReB_2 as 48.0 ± 5.6 GPa under the load of 0.49 N, Locci *et al.*[25] measured the hardness in the interval 31.1 - 20.7 GPa depending on the applied indentation load (0.49–4.9 N), and Dubrovinskaia *et al.*[23] measured the hardness less than 40 GPa (superhardness limit) in their technical comment on the study of Chung *et al.*[17] In another recent experiment, Vickers microhardness was measured by Otani *et al.*,[26] for their produced material (ReB_2). Using self-propagation high-temperature reaction techniques by Otani *et al.*, the measurements were carried out on two different planes. Their hardness results decreased from 30.8 to 19.8 GPa and from 35.8 to 14.3 GPa (in different planes) while decreasing temperature from 20 to 1000 °C, respectively.

However, in the theoretical studies which are based on the atomic properties and bond strengths, Simunek[51] calculated the hardness of ReB_2 as 35.8 GPa, and, Zhou *et al.*[30] calculated the same hardness as 46.0 GPa by the same method but they used the different reference energies for Re and B. On the other hand, Chen *et al.*[27] estimated the hardness as 47.5 (45.5) GPa with LDA (GGA) approximations. As it can be seen in Table V, the present theoretical result for hexagonal structure of ReB_2 is 35.9 GPa, agree well with the Simunek's

TABLE IV. The calculated elastic constants (in GPa) and the shear anisotropy ratio (A) of MnB_2, TcB_2, and ReB_2.

Compound	c_{11}	c_{33}	c_{44}	c_{66}	c_{12}	c_{13}	A
MnB_2	508	895	278	169	170	99	1.65
TcB_2	595	937	251	227	142	96	1.11
	579[a]	949[a]	248[a]	212[a]	156[a]	114[a]	
ReB_2	675	1081	278	264	147	115	1.05
	643[a]	1035[a]	263[a]	244[a]	159[a]	129[a]	1.03[d]
	716[b]	1108[b]	290[b]	266[d]	151[b]	133[b]	
	679[c]	1083[c]	284[c]		170[c]	137[c]	
	668[d]	1063[d]	273[d]		137[d]	147[d]	

[a]Reference 28.
[b]Reference 29.
[c]Reference 29 with SOC+relaxed.
[d]Reference 31.

TABLE V. The calculated Voigt (B_V) and Reuss (B_R) Bulk moduli, the Voigt (G_V), and Reuss (G_R) shear moduli in GPa, Young modulus (E, in GPa), Vickers Hardness (H, in GPa), the G/B, and Poisson ratio (v) for the hexagonal structures of MnB_2, TcB_2, and ReB_2.

Compound	B_V	B_R	B	G_V	G_R	G	E	H	G/B	v
MnB_2	294.2	283.5	288.9	247.8	226.9	237.3	558.9	43.9	0.82	0.18
TcB_2	310.7	302.0	306.3	265.1	255.3	260.2	608.4	37.0	0.85	0.17
			314[a]			277[a]	704[a]		0.88[a]	0.21[a]
ReB_2	353.9	341.5	347.7	300.8	290.0	295.4	690.6	35.9	0.85	0.17
	362.4[k]	346.7[k]	344[a]	293.5[k]	285.2[k]	304[a]	642[a]	48.0[d]	0.88[a]	0.21[a]
			359[b]			310[b]	725[b]	35.8[f]		0.17[b]
			356[c]			293[c]	691[c]	46.0[g]		0.18[c]
			360[d]			298[e]	682.5[k]	45.2[h]		0.18[k]
			360[e]			289.4[k]		31.1[i]		
			354.5[k]					30.8[j]		

[a]Reference 28.
[b]Reference 29.
[c]Reference 29 with SOC+relaxed.
[d]Reference 17.
[e]Reference 32.
[f]Reference 51.
[g]Reference 30.
[h]Reference 27.
[i]Reference 25.
[j]Reference 26.
[k]Reference 31.

result (35.8 GPa), but less than the other theoretical result.[30] These present results are within the experimental results [Less than the result of Chung *et al.*[17] (~30%) and higher than the result of Locci *et al.*[25] (~16%), respectively. There is a large difference between both experimental data.]. The large difference in experimental results is not surprise. Because, the experimental techniques are completely different in both steps of synthesizes and hardness measurements of ReB_2. In addition to the effect of hardness anisotropies,[41] it may be a stoichiometric problem due to, and during the experiments combustion and/or polycrystallization reactions of the material to take probably progress. Furthermore, in the measuring of hardness, orientation properties of the indentations and/or applied different loads on indenters in a specific time may affect the results. However, experimental average hardness values of Chung *et al.*[17] and directionally hardness of Otani *et al.*[26] were measured within orientations of grains, and the values of Locci *et al.*[25] were obtained as without indicating of orientations. We point out that in the hexagonal structure of ReB_2, the incompressibility of c axis is very high (see Fig. 5) and the short distances are take place between Re and B, and, B and B atoms in the (110) plane. Also, all antibonding populations, located on the bonds of B–B and Re–B are directionally, along the c axis, perpendicular to (00l) planes (see Table II). On the other hand, we obtained the highest bond strengths as 0.207 for Re–B bonds (d =2.206 Å) and 0.188 for B–B bonds (d=1.805 Å) for ReB_2, which are in (110) plane and they might strongly be responsible from the hardness of the material. Our calculations show that these are not the highest ones in all three structures, the highest values are 0.228 for four Mn–B bonds (d=2.086 Å), and 0.195 for six B–B bonds (d=1.744 Å) in MnB_2 structure. Here, it should be remembered that diamond is known the hardest material, the hardness of single-crystal diamond varies from about 70–120 GPa, depending on the crystallographic plane and direction of indentations.[63] So, average experimental results of Chung *et al.*[17] might have been predominant in parallel to highly directional bonds and which may result in scratching marks on a diamond surface.

Now, let us consider why the results of three theoretical calculations are different, although all three have used the same method. We note that the method is applied to ReB_2-type MnB_2, TcB_2, and ReB_2 structures, as that of Simunek's used in Ref. 51. Simunek and we calculate the reference energies ($e_i=Z_i/R_i$) by using atomic radii which are taken from the metallic structure of the elements,[54] because all three of materials which are studied here are in metallic character. Hence, the reference energies for the individual atoms were calculated as 4.364, 4.412, 4.747, and 3.061 eV for Re, Tc, Mn and B, respectively. But, in Ref. 30 the reference energies for Re and B atoms were calculated as 4.878 and 3.09 eV, respectively.

As indicated in Ref. 51, the hardness depends on the atomic radius and the number of nearest neighboring of the atoms. Therefore, these dependences for true hardness of the materials may have given higher than the calculated ones if the atomic radii are taken from pure metallic structures. Our calculations show that although hexagonal structures of ReB_2-type TcB_2 and ReB_2 are hard materials, hardness are ~37 GPa and ~36 GPa, respectively, the hexagonal structure of MnB_2 is superhard (~44 GPa) which is more than superhardness limit (40 GPa). However, even though the structures of TcB_2 and ReB_2 are known to be superhard or potential superhard materials, up to now, there is no calculated hardness data yet (to the knowledge of authors) for the ReB_2-type MnB_2 at the equilibrium geometry and at 0 GPa pressure.

To further explanation of the hardness and compressibility, we present graphs of the lattice constants, axial ratios,

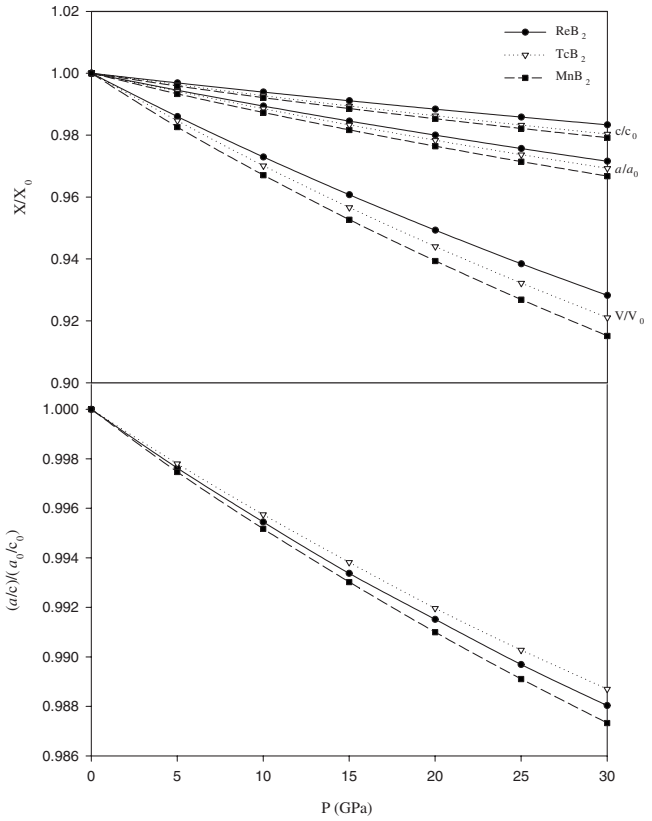

FIG. 5. (a) The calculated lattice axis and volumetric compressions, and (b) normalized axial ratios as a function of hydrostatic pressure of MnB_2, TcB_2, and ReB_2.

and volumes of MnB_2, TcB_2, and ReB_2 as a function of pressure. As it can be seen from the Fig. 5, all three structures are more compressible along a axis than c axis, and they are also volumetric compressible materials. The shear anisotropy ratio values are also proved this idea (see Table IV). As seen from the Fig. 5, although they are all ultraincompressible materials, the lattice parameters (a and c) and also volume (Ω) of MnB_2 are more compressible than that of TcB_2 and ReB_2. These results suggested that antibonding interactions between boron and transition metal atoms occur along the c axis [in the (110) planes], these leading to highly directional repulsive electronic interactions, and the least compressibility in the c direction.

The calculated sound velocities and Debye temperatures of MnB_2, TcB_2, and ReB_2, are tabulated in Table VI. As seen in Table VI, the Debye temperature and the sound velocity in the MnB_2 structure are higher than that of TcB_2 and ReB_2. Thus, according to the theory of Abrahams and Hsu[57] (see their empirical relation, Eq. (10)), and also conclusions of Hao *et al.*,[31] these results support that MnB_2 should be harder than TcB_2 and ReB_2.

TABLE VI. The calculated density (in g/cm^3), transverse (v_t), longitudinal (v_l), and average (v_m) sound velocities (in m/s) calculated from polycrystalline bulk and shear modulus, and Debye temperature (in K) of MnB_2, TcB_2, and ReB_2.

Compound	ρ	v_t	v_l	v_l	θ_D
MnB_2	5.510	6562.9	10480.8	7228.2	1090.2
TcB_2	7.522	5881.7	9319.3	6472.3	930.9
ReB_2	12.952	4775.6	7566.6	5255.2	755.5
					858.3[a]

[a]Reference 31.

IV. CONCLUSIONS

In conclusion, we have presented first-principle investigations of the structural, electronic and mechanical properties of hexagonal MnB_2, TcB_2, and ReB_2 crystal structures. Our calculations show that the ReB_2-type hexagonal structures of MnB_2, TcB_2, and ReB_2 are energetically favorable than those of AlB_2-type structures. MnB_2 has the lowest-density and the lowest-lattice volume at equilibrium geometry, and mechanically more stable than TcB_2 and ReB_2 structures. It is interesting that MnB_2 has the lowest bulk modulus and also shear modulus, but the shortest bond length and the highest bond population and shear anisotropy ratio in all three of structures. Furthermore, we have also demonstrated that the other characteristic properties such as DOSs of valance band, the Debye temperature, transverse and longitudinal sound velocities of MnB_2 are different from that of TcB_2 and ReB_2. Calculated hardness of MnB_2 is higher than superhardness limit (40 GPa), i.e., it may be considered as a superhard material.

Thus, generally speaking on the contradiction of hardness of ReB_2, instead of weakness of the methods, it might be come from the structural, polycrystalline, and/or stoichiometric properties of the grains, orientations of indentation, applied load, and the specific time effects of the sample during the experiments. Finally, all three of structures within ReB_2-type have not magnetic moment, only MnB_2 within AlB_2-type hexagonal structure has finite magnetic moment at the equilibrium geometry. We hope that although AlB_2-type is well-known for a long time, ReB_2-type of hexagonal MnB_2 can be synthesized under certain extreme conditions as ReB_2.

The authors are grateful to Ş. Erkoç (from Phys. Dep. of METU) for carefully reading of the manuscript and also thank to B. Inem, (Head of Mechanical Metallurgy Section, Gazi Univ.) stimulating discussion. This work is supported by the State of Planning Organization of Turkey under Grant No. 2001K120590.

[1] S.-H. Jhi, J. Ihm, S. G. Louie, and M. L. Cohen, Nature (London) **399**, 132 (1999).
[2] J. Haines, J. M. Leger, and G. Bocquillon, Annu. Rev. Mater. Res. **31**, 1 (2001).
[3] E. Gregoryanz, C. Sanoup, M. Somayazulu, J. Badro, G. Fiquet, H.-K. Mao, and R. J. Hemley, Nature Mater. **3**, 294 (2004).
[4] R. B. Kaner, J. J. Gilman, and S. H. Tolbert, Science **308**, 1268 (2005).
[5] J. J. Gilman, R. W. Cumberland, and R. B. Kaner, Int. J. Refract. Met. Hard Mater. **24**, 1 (2006).
[6] R. W. Cumberland *et al.*, J. Am. Chem. Soc. **127**, 7264 (2005).
[7] H. Y. Gou, L. Hou, J. W. Zhang, H. Li, G. F. Sun, and F. M. Gao, Appl. Phys. Lett. **88**, 221904 (2006).
[8] Z. Y. Chen, H. J. Xiang, J. Yang, J. G. Hou, and Q. S. Zhu, Phys. Rev. B **74**, 012102 (2006).
[9] S. Chiodo, H. J. Gotsis, N. Russo, and E. Sicilia, Chem. Phys. Lett. **425**, 311 (2006).
[10] U. Lundin, L. Fast, L. Nordstrom, B. Johansson, J. M. Wills, and O. Eriksson, Phys. Rev. B **57**, 4979 (1998).
[11] Z. Wu, X.-J. Chen, V. V. Struzhkin, and R. E. Cohen, Phys. Rev. B **71**, 214103 (2005).
[12] J. S. Tse, D. D. Klug, K. Uehara, Z. Q. Li, J. Haines, and J. M. Leger, Phys. Rev. B **61**, 10029 (2000).
[13] C. Z. Fan *et al.*, Phys. Rev. B **74**, 125118 (2006).
[14] H. Cynn, J. E. Klepeis, C. S. Yoo, and D. A. Young, Phys. Rev. Lett. **88**, 135701 (2002).
[15] J. C. Crowhurst, A. F. Goncharov, B. Sadigh, C. L. Evans, P. G. Morrall, J. L. Ferreira, and A. J. Nelson, Science **311**, 1275 (2006).
[16] A. F. Young, C. Sanloup, E. Gregoryanz, S. Scandolo, R. J. Hemley, and H.-K. Mao, Phys. Rev. Lett. **96**, 155501 (2006).
[17] H. Y. Chung, M. B. Weinberger, J. B. Levine, A. Kavner, J. M. Yang, S. H. Tolbert, and R. B. Kaner, Science **316**, 436 (2007).
[18] M. Zhang, M. Wang, T. Cui, Y. Ma, Y. Niu, and G. Zou, J. Phys. Chem. Solids **69**, 20096 (2008).
[19] J. C. Zheng, Phys. Rev. B **72**, 052105 (2005).
[20] Z. W. Chen *et al.*, Phys. Rev. B **75**, 054103 (2007).
[21] X. Hao, Y. Xu, Z. Wu, D. Zhou, X. Liu, and J. Meng, J. Alloys Compd. **453**, 413 (2008).
[22] A. Simunek and J. Vackar, Phys. Rev. Lett. **96**, 085501 (2006).
[23] N. Dubrovinskaia, L. Dubrovinsky, and V. L. Solozhenko, Science **318**, 1550c (2007).
[24] H. Y. Chung, M. B. Weinberger, J. B. Levine, R. W. Cumberland, A. Kavner, J. M. Yang, S. H. Tolbert, and R. B. Kaner, Science **318**, 1550d (2007).
[25] A. M. Locci, R. Licheri, R. Orru, and G. Cao, Ceram. Int. **35**, 397 (2009).
[26] S. Otani, M. M. Korsukova, and T. Aizawa, J. Alloys Compd. **477**, L28 (2009).
[27] X.-Q. Chen, C. L. Fu, M. Krcmar, and G. S. Painter, Phys. Rev. Lett. **100**, 196403 (2008).
[28] Y. X. Wang, Appl. Phys. Lett. **91**, 101904 (2007).
[29] Y. Liang and B. Zhang, Phys. Rev. B **76**, 132101 (2007).
[30] W. Zhou, H. Wu, and T. Yildirim, Phys. Rev. B **76**, 184113 (2007).
[31] X. Hao, Y. Xu, Z. Wu, D. Zhou, X. Liu, X. Cao, and J. Meng, Phys. Rev. B **74**, 224112 (2006).
[32] X. Zhu, D. Li, and X. Cheng, Solid State Commun. **147**, 301 (2008).
[33] M. Wang, Y. Li, T. Cui, Y. Ma, and G. Zou, Appl. Phys. Lett. **93**, 101905 (2008).
[34] R. Kiessling, Acta Chem. Scand. **4**, 146 (1950).
[35] I. Binder, Acta Crystallogr. **13**, 356 (1960).
[36] L. Andersson, B. Dellby, and H. P. Myers, Solid State Commun. **4**, 77 (1966).
[37] E. Legrand and S. Neov, Solid State Commun. **10**, 883 (1972).
[38] A. Cely, L.-E. Tergenius, and T. Lundstrom, J. Less-Common Met. **61**, 193 (1978).
[39] D. R. Armstrong, Theor. Chim. Acta **64**, 137 (1983).
[40] P. Vajeeston, P. Ravindran, C. Ravi, and R. Asokamani, Phys. Rev. B **63**, 045115 (2001).
[41] M. D. Segall, P. J. D. Lindan, M. J. Probert, C. J. Pickard, P. J. Hasnip, S. J. Clark, and M. C. Payne, J. Phys.: Condens. Matt. **14**, 2717 (2002).
[42] J. P. Perdew, J. A. Chevary, S. H. Vosko, K. A. Jackson, M. R. Pederson, D. J. Singh, and C. Fiolhais, Phys. Rev. B **46**, 6671 (1992).
[43] J. P. Perdew, K. Burke, and M. Ernzerhof, Phys. Rev. Lett. **77**, 3865 (1996).
[44] D. Vanderbilt, Phys. Rev. B **41**, 7892 (1990).
[45] D. M. Ceperley and B. J. Alder, Phys. Rev. Lett. **45**, 566 (1980).
[46] S. J. La Placa and B. Post, Acta Crystallogr. **15**, 97 (1962).
[47] S. Khmelevskyi and P. Mohn, Solid State Commun. **113**, 509 (2000).
[48] S. Q. Wu, Z. F. Hou, and Z. Z. Zhu, Solid State Commun. **143**, 425 (2007).
[49] R. Hill, Proc. Phys. Soc. **65**, 349 (1952).
[50] S. G. Roberts, P. D. Warren, and P. B. Hirsch, in *Science of Hard Materials-3*, Proceedings of the Third International Conference on the Science of Hard Materials, edited by V. K. Sarin (Elsevier, London, 1987), p. 19.
[51] A. Simunek, Phys. Rev. B **75**, 172108 (2007).
[52] F. Gao, J. He, E. Wu, S. Liu, D. Yu, D. Li, S. Zhang, and Y. Tian, Phys. Rev. Lett. **91**, 015502 (2003).
[53] F. M. Gao, R. Xu, and K. Liu, Phys. Rev. B **71**, 052103 (2005).
[54] W. B. Pearson, *The Crystal Chemistry and Physics of Metals and Alloys* (Wiley, NewYork, 1972), p. 151, Table 4.4.
[55] P. Ravindran, L. Fast, P. A. Korzhavyi, B. Johnnsson, J. Wills, and O. Eriksson, J. Appl. Phys. **84**, 4891 (1998).
[56] D. B. Sirdeshmukh, L. Sirdeshmukh, and K. G. Subhadra, *Micro- and Macro-Properties of Solides: Thermal, Mechanical and Dielectric Properties*, Springer Series in Material Science (Springer, New York, 2006), Vol. 80, p. 315.
[57] S. C. Abrahams and F. S. L. Hsu, J. Chem. Phys. **63**, 1162 (1975).
[58] M. D. Segall, R. Shah, C. J. Pickard, and M. C. Payne, Phys. Rev. B **54**, 16317 (1996).
[59] M. C. Cadeville, J. Chem. Solids **27**, 667 (1966).
[60] M. Kasaya and T. Hihara, J. Phys. Soc. Jpn. **29**, 336 (1970).
[61] J.-H. Xu, T. Oguchi, and A. J. Freeman, Phys. Rev. B **35**, 6940 (1987).
[62] J.-H. Xu and A. J. Freeman, Phys. Rev. B **40**, 11927 (1989).
[63] C. A. Brookes and E. J. Brookes, Diamond Relat. Mater. **1**, 13 (1991).
[64] M. Born, Proc. Cambridge Philos. Soc. **36**, 160 (1940).
[65] J.-Y. Wang and Y.-C. Zhou, Phys. Rev. B **69**, 144108 (2004).